

RAL-TR-1998-037
DTP/98/32
Cavendish-HEP-97/12
August 1998
Revised December 1998

Spin correlations in $e^+e^- \rightarrow 4$ jets¹

S. Moretti^{a,2} and W.J. Stirling^{b,c}

*a) Rutherford Appleton Laboratory,
Chilton, Didcot, Oxon OX11 0QX, UK.*

*b) Department of Physics, University of Durham,
South Road, Durham DH1 3LE, UK.*

*c) Department of Mathematical Sciences, University of Durham,
South Road, Durham DH1 3LE, UK.*

Abstract

Existence of discrepancies between experimental data and Monte Carlo predictions for angular distributions in four-jet production via e^+e^- annihilation has been known for some time at LEP1. As such QCD processes constitute significant backgrounds to $e^+e^- \rightarrow W^+W^- \rightarrow 4$ -jet production at LEP2, we consider the possibility that an erroneous modelling of the helicity structure of the final-state partons could affect the accuracy of experimental measurements of the W^\pm boson parameters.

¹E-mails: Moretti@rl.ac.uk; W.J.Stirling@durham.ac.uk.

²Formerly: Cavendish Laboratory, Cambridge University, Madingley Road, Cambridge CB3 0HE, UK.

1 Introduction and motivation

The partonic reactions $e^+e^- \rightarrow q\bar{q}gg$ and $e^+e^- \rightarrow q\bar{q}Q\bar{Q}$ (see Fig. 1) constitute the dominant (lowest-order) component of the annihilation rate of electrons and positrons into four jets. They represent a benchmark process in QCD phenomenology at present and future e^+e^- colliders for several reasons.

First, they provide a test of the underlying $SU(N_C)$ colour symmetry of the strong interactions between quarks and gluons, as the cross section is sensitive to the three fundamental colour factors C_A , C_F (the Casimir operators of the fundamental and adjoint representations of the gauge group $SU(N_C)$, respectively) and T_F (the normalisation of the generators of the fundamental representation). These are determined from the $SU(N_C)$ generators $(T^a)_{ij}$ and the structure constants f^{abc} via the relations

$$\sum_{a,b} f^{abc} f^{abd^*} = \delta^{cd} C_A, \quad \sum_a (T^a T^{a\dagger})_{ij} = \delta_{ij} C_F, \quad \text{Tr}[T^a T^{b\dagger}] = \delta^{ab} T_F, \quad (1)$$

where $a, b, \dots (i, j, \dots)$ represent gluon(quark) colour indices, yielding

$$C_A = N_C, \quad C_F = (N_C^2 - 1)/2N_C, \quad T_F = 1/2. \quad (2)$$

In QCD (i.e. $N_C = 3$) one has $C_A = 3$ and $C_F = 4/3$. The factors C_A , C_F and T_F represent the relative strength of the couplings (squared) of the processes $q \rightarrow qg$, $g \rightarrow gg$ and $g \rightarrow q\bar{q}$, respectively (see for example Ref. [1]).

Second, under the assumption that $SU(N_C \equiv 3)$ is indeed the gauge group of the theory, a measurement of these colour factors (in particular of $T_R = N_F T_F$) can be converted into a constraint on the value of the number of quark flavours active at the energy scale at which the e^+e^- annihilation takes place. For example, N_F would be increased (by approximately 3) from its ($N_F = 5$) Standard Model (SM) value at LEP by an additional New Physics contribution from very light gluinos \tilde{g} [2] produced in the process $e^+e^- \rightarrow q\bar{q}\tilde{g}\tilde{g}$ via a $g^* \rightarrow \tilde{g}\tilde{g}$ splitting [3].

Third, QCD four-jet production forms a significant background to $e^+e^- \rightarrow W^+W^- \rightarrow 4$ jets at LEP2 [4], for both the ‘threshold’ (total cross section) and the ‘direct reconstruction’ (W^\pm line shape) methods employed in the measurement of M_W , even after the implementation of typical W^\pm selection cuts [5]. Indeed, although biased by systematic uncertainties due to relatively unknown ‘Bose-Einstein’ [6] and ‘colour interconnection’ [7]

effects, the fully hadronic signature of the two W^\pm s still represents to date the experimentally preferred decay channel, because kinematic constraints can tighten the precision of the M_W measurement.

Fourth, four-jet events represent a serious background in the search for Higgs particles at LEP2 [8] and beyond (e.g. at the Next Linear Collider [9]) [10], both in the standard electroweak (EW) theory and in possible extensions. In the SM, the dominant Higgs production channel proceeds via the ‘bremsstrahlung’ process $e^+e^- \rightarrow Z\phi$ [11], followed by the hadronic decays $\phi \rightarrow b\bar{b}$. In this respect, it should be recalled that Z bosons have a 70% branching ratio into a pair of jets. Such arguments also apply to the case of the light h and heavy H Higgs scalars of the Minimal Supersymmetric Standard Model (MSSM) [12]. In addition, in the MSSM four-jet signatures arise naturally from the decays of the h scalar and the A pseudoscalar produced in pairs via $e^+e^- \rightarrow hA$ [12].

Fifth, the four-jet channel could well be the footprint of new *sparticles* at LEP2 or beyond, via the production of two resonances both decaying hadronically. In this context, it should be recalled that the production of several different types of supersymmetric particles was advocated some years ago as an explanation of the apparent excess of four-jet events as recorded by the ALEPH Collaboration [13]. For example, pairs of sneutrinos [14], squarks [15] (in particular sbottoms [16]), charginos and neutralinos [17, 18, 19, 20] and also selectrons [21] can yield four-jet signatures. Technicolour was also suggested as a possible explanation of the ALEPH events [22].

For all of the above reasons it is clearly very important that four-jet events are correctly implemented in the Monte Carlo (MC) programs which are widely used in phenomenological studies of hadron production at e^+e^- colliders (e.g. HERWIG [23], JETSET/PYTHIA [24], ARIADNE [25], etc.). In this connection, it is rather worrying that certain aspects of four-jet production are apparently *not* well described by the *standard* ‘ $\mathcal{O}(\alpha_s)$ ME + parton shower (PS)’ MC programs. For example, four-jet studies performed by the ALEPH Collaboration at LEP1 [26] have revealed a significant disagreement (up to 20% in some regions) between data and MCs for distributions in the four-jet angular variables: (i) the Bengtsson-Zerwas angle χ_{BZ} ; (ii) the Körner-Schierholz-Willrodt angle Φ_{KSW} ; (iii) the (modified) Nachtmann-Reiter angle θ_{NR}^* ; (iv) the angle between the two least energetic jets θ_{34} . This is well illustrated by Fig. 2 of Ref. [26].

The above angular quantities are defined in terms of the four-momenta of the particles in the final state and are particularly sensitive to the flavour (fermionic and bosonic) com-

position of four-jet events, in the sense that the different spins carried by quarks and gluons induce very different relative orientations between the two planes defined by the directions of the *primary* (i.e. from the $\gamma^*, Z^{(*)}$ -splitting) and *secondary* (i.e. from the virtual gluon splitting into quarks or gluons) parton pairs³. For this reason, the angles χ_{BZ} , Φ_{KSW} , θ_{NR}^* and θ_{34} have profitably been used to fit the theoretical predictions to the data in order to measure the three colour factors C_A , C_F and T_F . It can therefore be argued that the disagreement might be evidence that the MCs do not provide a correct description of the spin correlations among the various partons over the all phase space. Conversely, $\mathcal{O}(\alpha_s^2)$ ME programs (for example, the ‘ $\mathcal{O}(\alpha_s^2)$ ME + string fragmentation model’ as implemented in JETSET, i.e. with no parton shower) yield a much better angular description of four-jet final states (see Fig. 3 of [26] and [28]). Indeed, all spin correlations are naturally included in a full matrix element calculation (perturbative QCD predicts very specific orientations among the four final-state partons, see for example Ref. [29]), but they are not necessarily present in a PS emulation of the four-jet final state, though their availability (in the infrared limit, where soft and collinear correlations can be factorised in analytic form) is a feature of some of the above mentioned MC codes (for example, for the HERWIG implementation, see Refs. [30, 31]).

It might appear, therefore, that $\mathcal{O}(\alpha_s^2)$ ME programs are the preferred tool for analysing QCD four-jet production at LEP (and beyond). However, the problem here is that such ME models contain ‘ad-hoc’ hadronisation which is adjusted to give a good description of some LEP1 data [26] (see also Ref. [32]) but cannot be reliably extrapolated to higher (e.g. LEP2) energies. Furthermore, it is a well known fact that their description of the sub-jet structure is very poor (see Ref. [33] for an overview).

The deficiencies of these various approaches have been known for some time. Indeed, a general concern about, on the one hand, the inability of the standard MC programs to reproduce accurately four-jet angular quantities typical of parton level QCD and, on the other hand, the limitations of the ME implementation in quantifying hadronic multiplicities, already emerged at the time of the CERN LEP2 Workshop, see Ref. [34]. In this

³To be more precise, the angle θ_{34} was originally introduced to discriminate between the double bremsstrahlung (Fig. 1a–b) and triple-gluon-vertex (Fig. 1c) diagrams of the $q\bar{q}gg$ subprocess (see Ref. [27]), in order to provide direct proof of the non-Abelian structure of QCD. In fact, the variable θ_{34} is more sensitive to the gluon propagator singularity in the graphs of Fig. 1c, which is of course absent in those of Fig. 1a–b (see also the discussion in Sect. 3 below), than it is to spin correlations among partons.

respect, a key point not addressed there and that in our opinion deserves urgent attention is to assess whether or not also the angular behaviour of four-jet QCD events that survive W^+W^- selection criteria is poorly modelled by the standard parton showers, as well as to quantify the sort of differences that one should expect from the two approaches. While it is the purpose of this study to specifically address this question, we also attempt here to understand the source of the disagreement between the PS and the ME predictions for the above angular variables.

The plan of the paper is as follows. In the next Section we describe our method of computing four-jet rates using perturbative QCD. In Section 3 we present our results, and Section 4 contains a brief summary and some conclusions.

2 $e^+e^- \rightarrow q\bar{q}gg$ and $e^+e^- \rightarrow q\bar{q}Q\bar{Q}$ events

In order to generate the exact leading-order (LO) QCD predictions for the four-parton processes we use the FORTRAN codes already exploited in Refs. [35, 36, 37]. Such programs include not only all the angular correlations between primary and secondary partons, but also all quark masses and both the γ^* and $Z^{(*)}$ intermediate contributions. As numerical inputs for the electroweak parameters we take $\alpha_{em} = 1/128$ and $\sin^2\theta_W = 0.23$, while for the Z boson mass and width we use $M_Z = 91.1$ GeV and $\Gamma_Z = 2.5$ GeV, respectively. For the W^\pm boson, we use $M_W = 80.23$ GeV and $\Gamma_{W^\pm} = 2.08$ GeV. The u , d and s quarks are taken to be massless, while for c and b we take $m_c = 1.35$ GeV and $m_b = 4.95$ GeV. The strong coupling constant α_s has been computed at two-loop order (NLO), for $N_F = 5$ active flavours, with $\Lambda_{\text{QCD}} = 190$ MeV and scale choice $\mu = \sqrt{s}$, where \sqrt{s} is the centre-of-mass (CM) energy.

In order to define a four-jet sample we need to introduce a jet algorithm. In the present study we will use the so-called ‘Durham’ (D) one⁴ [39], which is widely used at LEP and SLD, based on the ‘measure’

$$y_{ij}^D = \frac{2 \min(E_i^2, E_j^2)(1 - \cos\theta_{ij})}{s}. \quad (3)$$

In the above equation E_i and E_j are the energies of the particles i and j , and θ_{ij} is their relative angle (with $i \neq j = 1, \dots, 4$). In our tree-level ME calculations, the four-jet

⁴See Ref. [38] for a survey of jet clustering algorithms and their properties.

cross section for a given algorithm is simply equal to the four-parton cross section with a cut $y_{ij} \geq y_{\text{cut}}$ on all possible parton pairs (ij) . In contrast, in our parton-shower studies, we need to define a jet clustering procedure as well. In these cases, we have adopted the so-called E-scheme, so that the four-momentum of a new cluster (or pseudoparticle) k is found from its constituents i and j by simple addition, $p_k = p_i + p_j$. The joining procedure is repeated until all pairs of clusters have a separation above y_{cut} . This final set of clusters is called jets.

At this point, we should further mention that we have also tried out three other jet clustering schemes, such as the ‘Jade’ [40], ‘Geneva’ [41] and ‘Cambridge’ [42] ones. Indeed, we have verified that none of our conclusions depends on the details of the jet algorithm used.

For completeness, we recall the definitions of the four angular variables [43, 44, 45, 46] introduced in the previous Section. One first orders the jets in energy such that $E_1 \geq E_2 \geq E_3 \geq E_4$. This way, one can identify the two most energetic jets with those originated by the quarks produced in the Z decay, and the other two with those produced in the g^* splitting (although such a procedure can be affected by systematic errors due to possible mis-assignments, see [47, 48]). Then, in terms of the three-momenta $\vec{p}_1, \dots, \vec{p}_4$ of the energy-ordered jets $1, \dots, 4$, the angles θ_{NR}^* , χ_{BZ} and θ_{34} are defined as

$$\theta_{\text{NR}}^* = \angle(\vec{p}_1 - \vec{p}_2, \vec{p}_3 - \vec{p}_4), \quad (4)$$

$$\chi_{\text{BZ}} = \angle(\vec{p}_1 \times \vec{p}_2, \vec{p}_3 \times \vec{p}_4), \quad (5)$$

and

$$\theta_{34} = \angle(\vec{p}_3, \vec{p}_4). \quad (6)$$

For Φ_{KSW} we actually use the ‘modified’ definition proposed in Ref. [48] (hereafter denoted by Φ_{KSW}^*), which is more sensitive than the original to the flavour composition (see Refs. [44, 48]). Thus, in events for which

$$|\vec{p}_1 + \vec{p}_3| > |\vec{p}_1 + \vec{p}_4| \quad (7)$$

we define

$$\Phi_{\text{KSW}}^* = \angle(\vec{p}_1 \times \vec{p}_3, \vec{p}_2 \times \vec{p}_4), \quad (8)$$

whereas in the opposite case we define Φ_{KSW}^* with \vec{p}_3 and \vec{p}_4 interchanged⁵.

⁵Note that the definition given in Eqs. (7)–(8) is equivalent to the original Φ_{KSW} angle [44] in events where the thrust axis is directed along $\vec{p}_1 + \vec{p}_3$ or $\vec{p}_1 + \vec{p}_4$.

3 Results

Our results are presented in Figs. 2–8 and in Tab. I. They include no Initial State Radiation (ISR) at any of the energies, neither in the ME nor in the PS calculations. This is done in order to simplify the discussion, as we have verified that the relative behaviours of the two implementations are unaffected by the inclusion of such emission. In addition, notice that in the course of our analysis we will at times modify the value of the jet resolution parameter y_{cut} adopted to define the four-jet sample. (In particular, the algorithm and the resolution used in Fig. 3 are the same as those of the ALEPH study [26], enabling us to make quantitative comparisons of our findings with the results given there.) This will help to illustrate the generality of the phenomenology that we will describe and, in particular, will help to distinguish properties of the underlying matrix elements from artifacts of the jet definition.

In the Introduction we argued that the disagreement between data and MCs could be due to a lack of adequate spin correlations among the partons generated in the phenomenological programs. In order to illustrate the sensitivity of the four angular variables to the helicity structure of the γ^* , $Z^{(*)}$ decay products we plot in Fig. 2 the distributions in χ_{BZ} , Φ_{KSW}^* , θ_{NR}^* and θ_{34} for the following subprocesses: (i) the four-quark component as obtained from the exact ME (tree-level) calculation; (ii) the same in a PS-like model obtained by averaging over the helicities of the virtual gluon in Fig. 1d (which removes the spin correlations between the two quark pairs in the final state); (iii) the triple-gluon-vertex component of two-quark-two-gluon events from the QCD ME (diagrams in Fig. 1c); (iv) the same in a PS-like model again simulated by averaging over the virtual gluon spins. Note that we have not presented similar distributions for the case of the double bremsstrahlung component of the two-quark-two-gluon ME (see Fig. 1a–b), for two reasons⁶. First, it is strongly suppressed (by roughly a factor $C_A/C_F = 9/4$ [29]) with respect to the triple-gluon-vertex contribution. Second, it is dominated by two infrared (i.e. soft and collinear) splittings of the virtual quarks into quark-gluon pairs, a dynamics which is well described by the PS implementation of the MC programs (as evidenced by their success in describing the phenomenology of $e^+e^- \rightarrow q\bar{q}g$ production [29]). In general, its angular behaviour is similar to that of the non-Abelian diagrams.

⁶See Ref. [48] for some typical distributions in the above angles for all the components of the $e^+e^- \rightarrow 4$ -parton process.

We emphasise that the results displayed in Fig. 2 (and also Fig. 4 below) should be regarded more as a useful exercise for understanding the underlying angular correlation properties of four-parton events in a ‘toy model’, rather than as a quantitatively reliable estimate of the relative behaviour of the exact QCD matrix elements vs. the MC parton shower description. In fact, two aspects should be noticed. First, the procedure of rewriting the diagrams in Fig. 1c and d as the product of the ME for $e^+e^- \rightarrow q\bar{q}g^*$ times those of the decays $g^* \rightarrow gg$ and $g^* \rightarrow Q\bar{Q}$, respectively, and of averaging over the spins of the intermediate state (so that the secondary $g^* \rightarrow gg$ and $g^* \rightarrow Q\bar{Q}$ splittings are azimuthally symmetric about the virtual gluon direction), differs in several respects from that implemented in the MC programs. For example, here the large-angle splitting is correctly reproduced whereas in MC programs only the collinear part is correctly represented. In contrast, in our example, the soft splitting is described only at lowest order whereas in the parton cascade higher order (logarithmically) enhanced terms are also included. Furthermore, as already mentioned in the Introduction, some of the most sophisticated MC programs do include azimuthal and polar correlations in the parton branching (in the soft and collinear limit), so that our toy model of PS should be further regarded as an extreme condition, and for this reason particularly useful for our purposes. Secondly, our procedure of separating the Abelian and non-Abelian components in the two-quark-two-gluon partonic MEs by simply retaining the amplitudes associated with Fig. 1a–b and 1c respectively, and neglecting their colour structure, is clearly non-gauge-invariant. However, we believe our distributions approximate quite accurately the true phenomenology of the four angular variables. In the first case, we do not expect the inclusion of large angle dynamics nor the neglect of logarithmically enhanced soft radiation to modify significantly the pattern of the angular correlations in the virtual gluon splitting. In the second respect, we stress that we have normalised all distributions to unity, since gauge invariance is more likely to affect the overall rates of the various components we have separated, rather than their angular shapes. We are therefore confident that the distributions shown in Fig. 2 (and 4) are an accurate representation of the behaviour produced by the corresponding diagrams in the full amplitude squared, and we can certainly use them as a guide to eventually pin-pointing the source of the discrepancies revealed in Ref. [26].

By looking at the χ_{BZ} distribution in Fig. 2, we see a clear peaking of the $q\bar{q}Q\bar{Q}$ component of the QCD ME around 90° , indicating the preference for the plane of the two secondary quark jets to be orthogonal to the plane of the two primary ones. In contrast, the

two secondary gluons from the triple-gluon vertex component prefer to be produced in the plane of the primary quark-antiquark pair (see also Fig. 9 of Ref. [49]). If in our toy model we switch off the angular correlations for the $q\bar{q}Q\bar{Q}$ final state we obtain a distribution that is significantly flatter, as expected. The ‘decorrelated’ version of the $q\bar{q}gg$ matrix element only including the triple-gluon-vertex diagrams gives a distribution similar to that of the decorrelated $q\bar{q}Q\bar{Q}$ model. The situation for the other three angular variables presented in Fig. 2, Φ_{KSW}^* , θ_{NR}^* and θ_{34} , is very much the same as for χ_{BZ} . That is, the two decorrelated versions of the QCD MEs are always significantly different from the ‘correct’ QCD ME predictions⁷.

Therefore, Fig. 2 clearly confirms the usefulness of the four angles in testing the underlying structure of the QCD processes in the presence of the full ME spin correlations. Conversely, if the described spin dynamics is not taken into account exactly, then their discriminating power between $q\bar{q}Q\bar{Q}$ and $q\bar{q}gg$ events could be significantly reduced. This should be especially borne in mind when contemplating high-precision QCD analyses such as those aiming to determine the C_A , C_F and T_F colour factors (and/or the possible existence of light gluinos).

For completeness, and in order to justify the confidence we have in our parton-level results, we also present in Fig. 3 the ratios between our ME and the PYTHIA results for the four angular distributions as obtained by adopting the same jet algorithm and resolution used in Ref. [26]. Here, in the MC implementation, partons are clustered before hadronisation until four jets are left. In addition, among all possible configurations of the latter, we only retain those for which the minimum of the y_{ij} measures is greater than y_{cut} . The aim is to reproduce here the salient features of Fig. 2 of Ref. [26], our ME outputs mimicking the data of that experimental study. In this respect, note that in Fig. 2 of Ref. [26] a full simulation (DYMU + JETSET + ALEPH detector) was performed and the angular variables were computed at hadron level. However, given the good agreement between the two figures, we believe that the main conclusions that we will draw from the forthcoming studies are unaffected by our simplification. We will now set aside further

⁷Note that in Fig. 2 of Ref [26] the distributions in the Bengtsson-Zerwas and (modified) Nachtmann-Reiter angles are ‘symmetrised’ by plotting with respect to $|\cos \chi_{\text{BZ}}|$ and $|\cos \theta_{\text{NR}}^*|$, respectively. This is because there exists an arbitrariness in the choice of the sign of the cosine of these angles. In contrast, in our Figs. 2 and 4 we have plotted the full angular range of the two variables, in order to gain more insight into the underlying problem of the parton shower implementation. Our distributions are not symmetric in themselves, since energy ordering of the jets is used (see for example the discussion in Ref. [48]).

considerations of the subject of precision QCD analyses and move on to another aspect of four-jet phenomenology.

We consider here the more topical issue of W^+W^- production and hadronic decays at LEP2. We have already mentioned that the QCD processes $e^+e^- \rightarrow \gamma^*, Z^{(*)} \rightarrow q\bar{q}gg, q\bar{q}Q\bar{Q}$ constitute significant backgrounds to $W^+W^- \rightarrow 4$ -jet production at LEP2, up to 20% of the signal depending on the event selection criteria used. Thus, it is crucial that the MC generators used in the experimental studies are able to correctly describe the salient features (that is, the overall rate and the differential distributions) of the QCD four-jet final states that are compatible with the $W^+W^- \rightarrow 4$ -jet kinematics.

A preliminary study of this problem was presented in Ref. [49]. In particular, it was investigated there whether QCD events which pass the W^+W^- event selection populate the ranges of the four-jet angular variables where the MCs have been shown to have problems describing the LEP1 data. Fig. 8 of Ref. [49], obtained from simulations of QCD and W^+W^- events at 172 GeV binned according to the four angular variables listed above, seemed to suggest that this is indeed the case. For example, using rather generic W^+W^- selection cuts, it was shown that the W^+W^- signal and the QCD background do cluster in the same angular regions. In particular, from Fig. 2 of Ref. [26] and Fig. 8 of Ref. [49], one can identify the following ranges of concern

$$|\cos \chi_{\text{BZ}}|, |\cos \theta_{\text{NR}}^*| < 0.7, \quad |\cos \Phi_{\text{KSW}}^*|, |\cos \theta_{34}| < 0.5. \quad (9)$$

Using the QCD predictions taken from PYTHIA and the W^+W^- predictions from KORALW [50], one finds that at LEP2 approximately half the QCD events have, for example, $|\cos \theta_{34}| < 0.5$, a region largely populated by the signal and where the JETSET PS fails to describe the LEP1 QCD data by up to 15% [28] !

It is therefore extremely important to investigate further such disagreement, particularly at LEP2 energies. For example, it is not impossible that W^+W^- selection cuts might somehow affect the relative performances of the ME and PS implementations in describing the spin correlations. In particular, the constraints devised to disentangle the W^+W^- signal at LEP2 could be such that the decorrelated MEs (and therefore also the MCs that they are supposed to emulate) approximate the exact results of the QCD MEs at LEP2 to a much better extent than they do at LEP1, thus reducing the severity of the problem.

Unfortunately, this possibility does not appear to be true, as can be deduced from Fig. 4. This shows the same distributions as Fig. 2, but now at $\sqrt{s} = 172$ GeV. In addition to the

processes studied at $\sqrt{s} = M_Z$ we now include the corresponding angular distributions obtained at parton level from the $e^+e^- \rightarrow W^+W^- \rightarrow q\bar{q}Q\bar{Q}$ ME introduced and described in Ref. [51]. As a ‘typical’ W^+W^- selection cut we have required $|M_{ij} - M_W| < 10$ GeV for at least two pairs of partons (ij). We see from Fig. 4 that, in the regions populated by W^+W^- events, the differences in the shapes of the ME and PS-like implementations are still significant for χ_{BZ} and Φ_{KSW}^* , somewhat reduced for θ_{NR}^* , and almost non-existent for θ_{34} . However, before claiming that θ_{34} has become a ‘safe’ quantity at LEP2, we should recall that, unlike the other variables, the angle between the two least energetic jets (generally, those produced in the virtual gluon splitting or by double gluon bremsstrahlung) is strongly dependent on the choice of the jet algorithm and/or the resolution parameter y_{cut} (i.e. on the higher-order terms of the perturbative expansion [52] not included here). As we have already mentioned, it is a direct measure of the singularity which appears when the two secondary partons become collinear. (This singularity is of course absent for the W^+W^- distribution, hence its flatness.) In other words, θ_{34} is a rather ‘infrared unstable’ variable that, in our opinion, is not a reliable indicator of the underlying properties of the QCD four-jet matrix elements.

Finally we turn to a comparison of the angular distributions at LEP2 obtained from the $\mathcal{O}(\alpha_s^2)$ QCD MEs and from two of the most widely used MC event generators, the up-to-date HERWIG 5.9 and PYTHIA 6.1, both of these using the ‘ $\mathcal{O}(\alpha_s)$ ME + PS’ approximation. We require them to reconstruct exactly four jets from the parton level before hadronisation, using the Durham jet finder with $y_{\text{cut}} = 0.002$. Fig. 5a shows the distributions in the four angular variables at the LEP2 energy of 172 GeV with the usual W^+W^- selection cut $|M_{ij} - M_W| < 10$ GeV enforced.

Even assuming that the overall normalisation is the same in all cases (the distributions in Fig. 5a are all normalised to unity), we see clear discrepancies between the ME (solid histogram) and PS (dashed and dotted histograms) predictions, although apparently less pronounced than at LEP1 (see Refs. [26, 28]). Furthermore, the discrepancies are significant in the regions where the W^+W^- signal peaks, especially for the Bengtsson-Zerwas and the (modified) Körner-Schierholz-Willrodt angles, well in line with our previous findings in the toy model. It is also evident that a simple rescaling of the distributions in the W^+W^- populated regions does not resolve the differences. To quantify the size of the effects seen in Fig. 5a, we reproduce in Tab. I (first line) the fraction of events found in various angular intervals (typically, around the maximum of the W^+W^- distributions) for

the ME predictions and those from HERWIG and PYTHIA. For reference, we also include the event fractions for the W^+W^- signal. From Tab. I we see that the differences between the QCD ME and the PS predictions can be up to about 10–15%⁸. In addition, HERWIG and PYTHIA behave rather similarly. Thus, we conclude that one should expect significant discrepancies in the shapes of the angular distributions predicted by the ME and PS models when performing $W^+W^- \rightarrow 4$ -jet analyses.

It is more difficult to draw any firm conclusions about possible differences in overall normalisation. The tree-level $\mathcal{O}(\alpha_s^2)$ ME four-jet *rate* is rather unstable against the effects of NLO QCD corrections (see Ref. [52]), with K -factors which can be of $\mathcal{O}(100\%)$. However, the *shape* of the angular distributions appears to be much more stable, implicitly demonstrating the relevance of the non-infrared dynamics in determining the behaviour of the four-jet angles. For example at LEP1, in the Durham algorithm and for $y = 0.008$ (the same set-up as in Ref. [26]), the typical K -factor of the angular spectra normalised to unity always lies in the range (1 ± 0.025) for all angular variables, see Figs. 1–4 of Ref. [53]. Therefore, NLO effects alone cannot account for the discrepancies seen in Fig. 2 of Ref. [26], nor do we expect them to be the reason for the differences noted in Fig. 5a here. For reference, we note that the JETSET LEP1 four-jet rates of [26] and [28] are obtained by using an acceptance-rejection algorithm such that the three-jet rate of the generated events matches that given by the $\mathcal{O}(\alpha_s)$ ME.

As we have mentioned the interplay between LO and NLO results in ME calculations, we would like to make one further comment. So far, we have compared the MEs at LO against the PS approximations of the MC programs, the latter defined by selecting exactly $n = 4$ jets with $y_{ij}^{\min} > y_{\text{cut}}$ (with $i \neq j = 1, \dots, 4$). Indeed, an alternative procedure which can be adopted to perform the comparison is to include also PS events with $n \geq 4$ jets (above the resolution) and eventually cluster these into exactly $n = 4$ jets. In fact, although the difference between the two approaches is next-to-leading and higher orders (recall that our ME are LO only), we have just mentioned that NLO effects do not alter the lowest order shapes of the MEs significantly (so should also be the case for NNLO, etc.). Furthermore, it is well known that in many cases summing over all possible radiation inclusively gives smaller ME/PS corrections than does vetoing resolvable radiation. Therefore, we present in Fig. 5b the usual angular distributions, now calculated from the two MCs in the new

⁸We have verified that the same size of effects are obtained using other jet algorithms and resolution parameters.

fashion. Indeed, the differences between the ME and the PS results are still sizable, as can be seen by looking at the second lines of Tab. I.

Therefore, at this point it seems clear that a PS implementation based on $\mathcal{O}(\alpha_s^2)$ QCD calculations for the hard scattering is needed in order to perform studies of four-jet events such as those outlined so far. In this respect, we note that an ‘ $\mathcal{O}(\alpha_s^2)$ ME + parton shower + cluster fragmentation’ option, based on both the correct second-order ME dynamics (from Refs. [55, 56]) of the partons and supplemented with the appropriate showering of the latter, thus avoiding the shortcomings of the ‘ $\mathcal{O}(\alpha_s^2)$ ME + fragmentation’ (i.e., without PS) approach, will soon be publicly available in the new HERWIG version 6.1 [54]⁹. The dashed curves in Fig. 3, showing the ratios of our ‘ $\mathcal{O}(\alpha_s^2)$ MEs’ to the HERWIG 6.1 ‘ $\mathcal{O}(\alpha_s^2)$ ME + PS’ implementation, at the parton level, well illustrates this improvement, allowing for residual differences between the two rates due to possible mis-assignments of the jet algorithm reconstructing the HERWIG parton shower backwards to the original four-parton state. The improvement is very much evident in the case of the angles χ_{BZ} , Φ_{KSW}^* and θ_{NR}^* . The only exception occurs for θ_{34} , where differences between the two approaches can still be relevant, especially when $\cos\theta_{34} \rightarrow 1$. However, this is not surprising, as we have already highlighted the sensitivity of this variable to higher-order effects in the collinear limit, which are indeed embodied in the PS evolution but not in the LO MEs (nor in the ‘ $\mathcal{O}(\alpha_s^2)$ ME + hadronisation’ model). Not surprisingly, the full NLO corrections to the shape of this angular distribution can be as large as 15%, again in the region $\cos\theta_{34} \rightarrow 1$, for example in the Cambridge scheme [53]. The appropriate treatment of such Sudakov effects due to soft-gluon emission [29] are beyond the scope of the present study and will be addressed elsewhere [54].

One might now wonder whether the above parton-level behaviours can survive the hadronisation process. We address this in Fig. 6, where the usual four angular distributions are plotted, but now at the *hadron* level (including both charged and neutral tracks in the jet reconstruction and allowing for the decays of the heavy hadrons), as obtained by HERWIG 6.1, using both $\mathcal{O}(\alpha_s)$ and $\mathcal{O}(\alpha_s^2)$ initiated PSs. From Fig. 6, it is evident that the soft dynamics of the hadronisation stage does not remove the partonic differences between the two approaches. Furthermore, by comparing Fig. 5a to Fig. 6, one can see that the discrepancies are of the same sort at the two QCD stages, being possibly larger at the hadron level in

⁹Some progress in the same direction as in HERWIG is being made also in the context of the PYTHIA environment [33].

the case of the Bengtsson-Zerwas angle. Therefore, it is more than plausible that ‘partonic’ angular effects are the source of the differences between the current PS MCs and the LEP1 data.

A very relevant issue which can be addressed at this point is whether such effects can influence the determination of physical parameters whose measurement depends on the estimation of the size and topology of the four-jet background from QCD. One important and topical example concerns the measurement of the W mass at LEP2, reconstructed from fully hadronic decays of W^\pm pairs, as discussed in the Introduction. However, in order to give quantitatively reliable estimates in this case, one should take into account various other non-trivial effects such as initial-state QED radiation, neutrinos that escape without detection, cracks in the detector acceptance, experimental resolution and efficiency, etc. In addition, we note that the various selection procedures for $W^+W^- \rightarrow 4$ -jet candidate events differ significantly from experiment to experiment. Therefore it is clear that a *full* study of the effect on the W mass can only be carried out within the context of a complete detector simulation, which is beyond the scope of this paper.

Nevertheless, we can address this issue here at a rather more modest level, to gauge the size of the effect. Thus, we run HERWIG once more to produce hadronic final states via the signal process $e^+e^- \rightarrow W^+W^- \rightarrow q\bar{q}Q\bar{Q}$ (IPROC=200, as in 5.9) and the background $e^+e^- \rightarrow \gamma^*, Z^* \rightarrow q\bar{q}gg, q\bar{q}Q\bar{Q}$, the latter generated both via $\mathcal{O}(\alpha_s)$ (IPROC=100, as in 5.9) and $\mathcal{O}(\alpha_s^2)$ (IPROC=600, new to 6.1) MEs. Again, we require exactly four jets to be reconstructed by means of the Durham scheme with $y_{\text{cut}} > 0.002$ and such that $|M_{ij} - M_W| < 10$ GeV for at least two pairs of jets (ij), but this time only within the angular regions typically populated by the signal. Following Fig. 5a, we have chosen the following constraints¹⁰:

$$|\cos \chi_{BZ}| > 0.5, \quad \cos \Phi_{\text{KSW}}^* < -0.5, \quad |\cos \theta_{\text{NR}}^*| > 0.5 \quad |\cos \theta_{34}| < 0.8. \quad (10)$$

Next, we plot an ‘average’ W^\pm mass, hereafter denoted by M_{ave} , for each event generated. There are several reasons for choosing the average rather than the two individual masses. For example, the mis-assignment of one particle from one W^\pm to the other reduces the first mass and increases the second, leaving the average less affected than each separately. In fact in each event there are three possible jet pairings, each giving one potential average W mass. Of these three, we exclude the one where the two most energetic jets are paired with

¹⁰Given the remark in Footnote 7, recall that we ought to symmetrize the cuts in the Bengtsson-Zerwas and Nachtmann-Reiter angles.

each other, since kinematically this is seldom the correct combination. The plot in Fig. 7 shows the shape of such a distribution for the three cases $\text{IPROC}=200$ (solid line), $\text{IPROC}=100$ (dashed line) and $\text{IPROC}=600$ (dotted line). From this figure the different shape of the two descriptions of the backgrounds is rather clear, particularly in the vicinity of the W^\pm mass resonance.

As a further step in our study we bin (see upper part of Fig. 8) the average W^\pm mass spectra as obtained by summing the signal and background rates, each with the appropriate normalisation as computed by HERWIG, in the two possible cases, depending on whether the $\mathcal{O}(\alpha_s)$ (dashed line) or the $\mathcal{O}(\alpha_s^2)$ (dotted line) MEs are used in the MC event generator to simulate the QCD noise. The ratio in each bin between the latter two distributions is shown in the lower plot of Fig. 8 (solid line). Indeed, the total spectra also differ significantly and the ratio between the two is not constant around M_W .

To investigate the possible consequences of the results shown in Figs. 7–8 on the determination of the W^\pm mass, we perform a MINUIT [57] fit on the two total distributions, with a fitting function of the form

$$f(m) = c_1 \frac{c_2^2 c_3^2}{(m^2 - c_2^2)^2 + c_2^2 c_3^2} + g(m) \quad (11)$$

where the term $g(m)$ is meant to simulate a smooth background due to mis-assigned jets induced by the clustering algorithm. For the latter, we adopt three different possible choices

$$g(m) = \begin{cases} 0, \\ c_4 + c_5 (m - c_2) + c_6 (m - c_2)^2, \\ c_4 \frac{1}{1 + \exp((m - c_5)/c_6)}, \end{cases} \quad (12)$$

that is, a null, a three-term polynomial and a smeared step function (motivated by the kinematical-limit shoulder at large masses). Note that in eq. (11) we have assumed a Breit-Wigner shape characterised by a peak height c_1 , a position c_2 and a width c_3 , corresponding to the normalisation, M_W and Γ_W , respectively, of the two distributions in Fig. 8.

To first approximation, then, the difference between the two values of the coefficient c_2 as obtained from fitting the two curves is a measure of the typical size of the systematic error that could be introduced in the experimental measurement of the W boson mass by a mis-modeling of the QCD four-jet background. We find this value to be around 10 MeV if we neglect altogether the intrinsic mis-assignment background or if we assume for the latter

a step function, whereas the difference somewhat decreases for a polynomial background, down to 2 MeV. Though not dramatically large, such numbers are nonetheless comparable to the expected size of the final systematic error on M_W from all other possible sources (as estimated for example at the LEP2 Workshop [4]) of about 50 MeV.

4 Summary and conclusions

In this paper we have investigated discrepancies in the predictions for distributions of typical four-jet angular variables obtained from matrix element and parton shower calculations. Comparison of the latter with LEP1 data from ALEPH revealed differences of up to 20%, while the ME calculations are in good agreement with the same sample. By constructing toy parton-shower models, using matrix elements in which the spin correlations between the secondary (i.e. from the g^* splitting) $Q\bar{Q}$ and gg pairs and the primary (i.e. from the $\gamma^*, Z^{(*)}$ decay) $q\bar{q}$ ones are switched off, we concluded that the source of the disagreement resides in the limited capability of the MC parton shower of reproducing the exact partonic spin correlations away from the infrared limit, if the ‘ $\mathcal{O}(\alpha_s)$ ME’ is used to generate the hard QCD scattering.

However, the main concern of our analysis was the impact that similar effects could have on four-jet studies at LEP2, in the context of $W^+W^- \rightarrow 4$ -jet phenomenology and W^\pm mass determinations. The preliminary exercises that we have carried out in this paper show that the shape of the angular distributions is not reproduced accurately by the MC parton showers at LEP2 either. Furthermore, these discrepancies survive even after the W^+W^- selection criteria are implemented as well as the hadronisation phenomenon.

It is possible, therefore, that at present the contribution of the QCD four-jet background is *not* being correctly simulated in candidate W^+W^- samples, and this could constitute a non-negligible source of error in the M_W determination at LEP2. We regard this as the most important conclusion of our paper, based on the fact that, after having performed a simple exercise to assess the size of such systematic error, we have found it to be as large as 10 MeV. This is of the same order as the foreseen precision on M_W at the end of the LEP2 runs. However, we stress that our estimate should not be taken too literally, since our study lacks many of the necessary ingredients of a complete simulation, such as detector effects, ISR, a more detailed background analysis (including all four-quark EW channels), etc., all of which is well beyond the scope of this paper.

Nonetheless, it is evident that it is of crucial importance that a dedicated implementation based on $\mathcal{O}(\alpha_s^2)$ QCD calculations is used in the MC simulations of four-jet samples of the type described in this paper. MC programs are now being upgraded to incorporate such second-order dynamics and we urge the experimental collaborations to adopt them in their analyses.

Acknowledgements

We are grateful to the UK PPARC for support, and to the Theoretical Physics Department at Fermilab for kind hospitality while part of this work was carried out. SM also thanks the Department of Theoretical Physics in Lund for hospitality, the Italian Institute of Culture ‘C.M. Lerici’ for a grant (Ref. #: Prot. I/B1 690) which supported his visit there, and T. Sjöstrand for useful conversations. Finally, we both thank Mike Seymour for carefully reading the manuscript and for useful comments, as well as for pointing out a mistake in our analysis and for performing detailed comparisons between the MEs used in this paper and those implemented in the new HERWIG version.

References

- [1] C. Quigg, ‘Gauge Theories of the Strong, Weak, and Electromagnetic Interactions’ (Benjamin-Cummings, 1983).
- [2] G.R. Farrar and P. Fayet, *Phys. Lett.* **B76** (1978) 575;
T. Goldman, *Phys. Lett.* **B78** (1978) 110;
I. Antoniadis, C. Kounnas and R. Lacaze, *Nucl. Phys.* **B211** (1983) 216;
M.J. Eides and M.J. Vytovsky, *Phys. Lett.* **B124** (1983) 83;
E. Franco, *Phys. Lett.* **B124** (1983) 271;
G.R. Farrar, *Phys. Rev. Lett.* **53** (1984) 1029;
S. Dawson, E. Eichten and C. Quigg, *Phys. Rev.* **D31** (1985) 1581;
J. Ellis and H. Kowalski, *Phys. Lett.* **B157** (1985) 437;
V. Barger, S. Jacobs, J. Woodside and K. Hagiwara, *Phys. Rev.* **D33** (1986) 57;
I. Antoniadis, J. Ellis and D.V. Nanopoulos, *Phys. Lett.* **B262** (1985) 109;
G.R. Farrar, *Phys. Lett.* **B265** (1991) 395.

- [3] P. Nelson and P. Osland, *Phys. Lett.* **B115** (1982) 407;
 B.A. Campbell, J. Ellis and S. Rudaz, *Nucl. Phys.* **B198** (1982) 1;
 G.L. Kane and W.B. Rolnick, *Nucl. Phys.* **B217** (1983) 117;
 B.A. Campbell, J.A. Scott and M.K. Sundareshan, *Phys. Lett.* **B126** (1983) 376.
- [4] Proceedings of the Workshop ‘Physics at LEP2’, eds. G. Altarelli, T. Sjöstrand and F. Zwirner, CERN Report 96-01.
- [5] Z. Kunszt and W.J. Stirling (conveners), in Ref. [4].
- [6] L. Lönnblad and T. Sjöstrand, *Phys. Lett.* **B351** (1995) 293.
- [7] G. Gustafson, U. Pettersson and P.M. Zerwas, *Phys. Lett.* **B209** (1988) 90;
 T. Sjöstrand and V.A. Khoze, *Phys. Rev. Lett.* **72** (1994) 28; *Z. Phys.* **C62** (1994) 281;
 G. Gustafson and J. Häkkinen, *Z. Phys.* **C64** (1994) 659.
- [8] M. Carena and P.M. Zerwas (conveners), in Ref. [4].
- [9] See for example: Proceedings of the Workshop ‘ e^+e^- Collisions at 500 GeV. The Physics Potential’, Munich, Annecy, Hamburg, 3–4 February 1991, ed. P.M. Zerwas, DESY 92–123A/B, August 1992, DESY 93–123C, December 1993.
- [10] P. Janot and P.M. Zerwas (conveners), in Ref. [9].
- [11] J.D. Bjorken, Proceedings of the ‘Summer Institute on Particle Physics’, *SLAC Report* 198 (1976);
 B.W. Lee, C. Quigg and H.B. Thacker, *Phys. Rev.* **D16** (1977) 1519;
 J. Ellis, M.K. Gaillard and D.V. Nanopoulos, *Nucl. Phys.* **B106** (1976) 292;
 B.L. Ioffe and V.A. Khoze, *Sov. J. Part. Nucl.* **9** (1978) 50.
- [12] J.F. Gunion and H.E. Haber, *Nucl. Phys.* **B278** (1986) 449.
- [13] ALEPH Collaboration, *Phys. Lett.* **B373** (1996) 246.
- [14] V. Barger, W.-Y. Keung and R.J.N. Phillips, *Phys. Lett.* **B364** (1995) 27.
- [15] G.R. Farrar, *Phys. Rev. Lett.* **76** (1996) 4115; *preprint* RU-95-82, December 1995.
- [16] A.K. Grant, R.D. Peccei, T. Veletto and K. Wang, *Phys. Lett.* **B379** (1996) 272.

- [17] D.K. Ghosh, R.M. Godbole and S. Raychaudhuri, *Z. Phys.* **C75** (1997) 357.
- [18] H. Dreiner, S. Lola and P. Morawitz, *Phys. Lett.* **B389** (1996) 62.
- [19] P.H. Chankowski, D. Choudhury and S. Pokorski, *Phys. Lett.* **B389** (1996) 677.
- [20] G.R. Farrar, *preprint* RU-96-71, August 1996.
- [21] M. Carena, G.F. Giudice, S. Lola and C.E.M. Wagner, *Phys. Lett.* **B395** (1997) 225.
- [22] S.F. King, *Phys. Lett.* **B381** (1996) 291.
- [23] G. Marchesini, B.R. Webber, G. Abbiendi, I.G. Knowles, M.H. Seymour and L. Stanco, *Comp. Phys. Commun.* **67** (1992) 465.
- [24] T. Sjöstrand, *Comp. Phys. Commun.* **39** (1984) 347;
M. Bengtsson and T. Sjöstrand, *Comp. Phys. Commun.* **43** (1987) 367.
- [25] L. Lönnblad, *Comp. Phys. Commun.* **71** (1992) 15.
- [26] ALEPH Collaboration, *Z. Phys.* **C76** (1997) 1.
- [27] See for example: P. Mättig, Proceedings of the Workshop ‘Photon Radiation from Quarks’, ed. S. Cartwright, Annecy, France, 2–3 December 1991, CERN Report 92-04.
- [28] G. Cowan, *J. Phys.* **G24** (1998) 307.
- [29] R.K. Ellis, W.J. Stirling and B.R. Webber, ‘QCD and Collider Physics’ (Cambridge University Press, 1996).
- [30] I.G. Knowles, *Nucl. Phys.* **B310** (1988) 571.
- [31] I.G. Knowles, *J. Phys.* **G17** (1991) 1562.
- [32] OPAL Collaboration, *Z. Phys.* **C65** (1995) 367.
- [33] J. André and T. Sjöstrand, *Phys. Rev.* **D57** (1998) 5767;
J. André, *preprint* LU-TP-97-12, June 1997, hep-ph/9706325.
- [34] I.G. Knowles and T. Sjöstrand (conveners), in Ref. [4].
- [35] A. Ballestrero, E. Maina and S. Moretti, *Phys. Lett.* **B294** (1992) 425.

- [36] A. Ballestrero, E. Maina and S. Moretti, *Nucl. Phys.* **B415** (1994) 265.
- [37] A. Ballestrero, E. Maina and S. Moretti, Proceedings of the ‘XXIXth Rencontres de Moriond: QCD and High Energy Hadronic Interactions’, Méribel, Savoie, France, 16/26 March 1994, ed. by J. Trân Thanh Vân, ed. Frontières, Gif-sur-Yvette, 1994, 367.
- [38] S. Moretti, L. Lönnblad, T. Sjöstrand, *JHEP* **08** (1998) 001.
- [39] Yu.L. Dokshitzer, contribution cited in the Report of the Hard QCD Working Group, Proc. Workshop on Jet Studies at LEP and HERA, Durham, December 1990, *J. Phys.* **G17** (1991) 1537.
- [40] JADE Collaboration, *Z. Phys.* **C33** (1986) 23;
JADE Collaboration, *Phys. Lett.* **B213** (1988) 235.
- [41] S. Bethke, Z. Kunszt, D.E. Soper and W.J. Stirling, *Nucl. Phys.* **B370** (1992) 310;
Erratum *preprint hep-ph/9803267*.
- [42] Yu.L. Dokshitzer, G.D. Leder, S. Moretti and B.R. Webber, *JHEP* **08** (1997) 001.
- [43] M. Bengtsson and P.M. Zerwas, *Phys. Lett.* **B208** (1988) 306.
- [44] J.G. Körner, G. Schierholz and J. Willrodt, *Nucl. Phys.* **B185** (1981) 365.
- [45] O. Nachtmann and A. Reiter, *Z. Phys.* **C16** (1982) 45.
- [46] M. Bengtsson, *Z. Phys.* **C42** (1989) 75.
- [47] S. Bethke, A. Ricker and P.M. Zerwas, *Z. Phys.* **C49** (1991) 59.
- [48] S. Moretti and J.B. Tausk, *Z. Phys.* **C69** (1996) 635.
- [49] A. Ballestrero *et al.*, *J. Phys.* **G24** (1998) 365.
- [50] M. Skrzypek, S. Jadach, W. Placzek and Z. Was, *Comput. Phys. Commun.* **94** (1996) 216.
- [51] V.A. Khoze, W.J. Stirling, S. Moretti, A. Ballestrero and E. Maina, *Z. Phys.* **C74** (1997) 493.

- [52] Z. Bern, L. Dixon, D.A. Kosower and S. Weinzierl, *Nucl. Phys.* **B489** (1997) 3;
Z. Bern, L. Dixon, D.A. Kosower, *Nucl. Phys.* **B513** (1998) 3;
L. Dixon and A. Signer, *Phys. Rev. Lett.* **D78** (1997) 811;
A. Signer, presented at the XXXIIInd Rencontres de Moriond ‘QCD and High-Energy Hadronic Interactions’, Les Arcs, France, 22-29 March 1997, SLAC *preprint* SLAC-PUB-7490, May 1997, [hep-ph/9705218](#);
E.W.N. Glover and D.J. Miller, *Phys. Lett.* **B396** (1997) 257;
J.M. Campbell, E.W.N. Glover and D.J. Miller, *Phys. Lett.* **B409** (1997) 503.
- [53] Z. Nagy and Z. Trócsányi, *Phys. Rev.* **D57** (1998) 5793.
- [54] G. Marchesini, B.R. Webber, I.G. Knowles, M.H. Seymour, G. Corcella, S. Moretti and K. Odagiri, in preparation.
- [55] R.K. Ellis, D.A. Ross and A.E. Terrano, *Nucl. Phys.* **B178** (1981) 421.
- [56] W.T. Giele and E.W.N. Glover, *Phys. Rev.* **D46** (1992) 1980.
- [57] F. James and M. Roos, *Comp. Phys. Commun.* **10** (1975) 343.

Table Caption

[I] Fraction of four-jet events in various angular intervals around the maxima of the W^+W^- distributions, as predicted by the: (i) ' $\mathcal{O}(\alpha_s^2)$ MEs' ($q\bar{q}gg + q\bar{q}Q\bar{Q}$), (ii) ' $\mathcal{O}(\alpha_s)$ ME + PS' (HERWIG, IPROC=100), (iii) ' $\mathcal{O}(\alpha_s)$ ME + PS' (PYTHIA, ISUB=1); and also, for reference, the ' $\mathcal{O}(\alpha_s^0)$ ME' for $e^+e^- \rightarrow W^+W^- \rightarrow q\bar{q}Q\bar{Q}$. All rates are obtained at parton level. The following cut has been implemented: $|M_{ij} - M_W| < 10$ GeV on at least two pairs of partons (ij). The CM energy is $\sqrt{s} = 172$ GeV. Results are shown for the Durham algorithm, with $y_{\text{cut}} = 0.002$. The first line refers to the case in which exactly $n = 4$ jets are reconstructed from the parton shower, while the second corresponds to $n \geq 4$, with the additional jets in the latter eventually clustered into four. (All n final tracks are above cut-off in both cases.)

Figure Captions

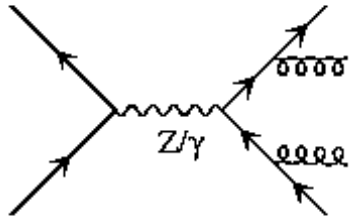
- [1] Feynman diagrams contributing in lowest order to QCD four-jet production in e^+e^- annihilation: (a,b) double-gluon-bremsstrahlung, (c) triple-gluon-vertex and (d) four-quark subprocesses.
- [2] Differential distributions for the following variables: (top-left) χ_{BZ} , (top-right) Φ_{KSW}^* , (bottom-left) $\cos\theta_{\text{NR}}^*$ and (bottom-right) $\cos\theta_{34}$ for the following subprocesses: four-quark in QCD (solid), four-quark in a PS-like model (dashed), triple-gluon in QCD (dotted), triple-gluon in a PS-like model (dot-dashed). The CM energy is $\sqrt{s} = M_Z$. All distributions are normalised to unity. Results are shown for the Durham algorithm, with $y_{\text{cut}} = 0.002$.
- [3] The ratio between the ME and PYTHIA implementation (solid) of the differential distributions for the following variables: (top-left) χ_{BZ} , (top-right) Φ_{KSW}^* , (bottom-left) $\cos\theta_{\text{NR}}^*$ and (bottom-right) $\cos\theta_{34}$. The default spin correlation matrices of the parton cascade in the MC program have been switched on. All distributions are at parton level. The CM energy is $\sqrt{s} = M_Z$. All distributions are normalised to unity. Results are shown for the Durham algorithm, with $y_{\text{cut}} = 0.008$. Exactly four jets are required to be reconstructed from the PYTHIA cascade. The corresponding ratio in case of HERWIG 6.1 is also shown (dashed): see later on.
- [4] Differential distributions for the following variables: (top-left) χ_{BZ} , (top-right) Φ_{KSW}^* , (bottom-left) $\cos\theta_{\text{NR}}^*$ and (bottom-right) $\cos\theta_{34}$ for the following subprocesses: four-quark in QCD (solid), four-quark in a PS-like model (dashed), triple-gluon in QCD (dotted), triple-gluon in a PS-like model (dot-dashed) and W^+W^- (shaded). The CM energy is $\sqrt{s} = 172$ GeV. All distributions are normalised to unity. The following cut has been implemented: $|M_{ij} - M_W| < 10$ GeV on at least two pairs of partons (ij). Results are shown for the Durham algorithm, with $y_{\text{cut}} = 0.002$.
- [5] Differential distributions for the following variables: (top-left) χ_{BZ} , (top-right) Φ_{KSW}^* , (bottom-left) $\cos\theta_{\text{NR}}^*$ and (bottom-right) $\cos\theta_{34}$ in case of ‘ $\mathcal{O}(\alpha_s^2)$ MEs’ ($q\bar{q}gg + q\bar{q}Q\bar{Q}$, solid histogram), ‘ $\mathcal{O}(\alpha_s)$ ME + PS’ (HERWIG, dashed histogram) and ‘ $\mathcal{O}(\alpha_s)$ ME + PS’ (PYTHIA, dotted histogram). The default spin correlation matrices of the parton cascade in the MC programs have been switched on. For reference, we also have

included the same spectra as obtained from the ‘ $\mathcal{O}(\alpha_s^0)$ ME’ for $e^+e^- \rightarrow W^+W^- \rightarrow q\bar{q}Q\bar{Q}$ (asterisk symbols). All distributions are at parton level. The following cut has been implemented: $|M_{ij} - M_W| < 10$ GeV on at least two pairs of partons (ij). The CM energy is $\sqrt{s} = 172$ GeV. Normalisation is to unity. Results are shown for the Durham algorithm, with $y_{\text{cut}} = 0.002$. (a) Exactly four jets are required to be reconstructed from the HERWIG and PYTHIA cascades. (b) At least four jets are required to be reconstructed from the HERWIG and PYTHIA cascades, eventually forced into exactly four.

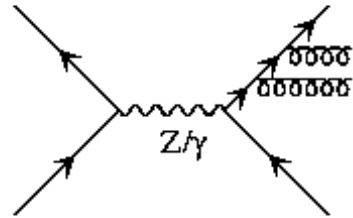
- [6] Differential distributions for the following variables: (top-left) χ_{BZ} , (top-right) Φ_{KSW}^* , (bottom-left) $\cos\theta_{\text{NR}}^*$ and (bottom-right) $\cos\theta_{34}$ in case of ‘ $\mathcal{O}(\alpha_s^2)$ ME + PS + Hadronisation’ (solid histogram) and ‘ $\mathcal{O}(\alpha_s)$ ME + PS + Hadronisation’ (dashed histogram), as obtained by using HERWIG. The default spin correlation matrices of the parton cascade in the two versions of the MC program have been switched on. The following cut has been implemented: $|M_{ij} - M_W| < 10$ GeV on at least two pairs of jets (ij), as defined at the hadron level. The CM energy is $\sqrt{s} = 172$ GeV. Normalisation is to unity. Results are shown for the Durham algorithm, with $y_{\text{cut}} = 0.002$. Exactly four jets are required to be reconstructed.
- [7] Differential distributions in the average W^\pm -mass (as defined in the text) for the W^+W^- signal (solid curve), the $\mathcal{O}(\alpha_s)$ (dashed curve) and the $\mathcal{O}(\alpha_s^2)$ (dotted curve) backgrounds (from HERWIG). Other than the constraint $|M_{ij} - M_W| < 10$ GeV on at least two pairs of jets (ij), as defined at the hadron level, the angular cuts of eq. (10) have also been implemented. The CM energy is $\sqrt{s} = 172$ GeV. Normalisation is to unity. Results are shown for the Durham algorithm, with $y_{\text{cut}} = 0.002$. Exactly four jets are required to be reconstructed.
- [8] Differential distributions (top) in the average W^\pm -mass (as defined in the text) for the sum of the W^+W^- signal and the $\mathcal{O}(\alpha_s)(\mathcal{O}(\alpha_s^2))$ background (from HERWIG): dashed(dotted) curve. Other than the constraint $|M_{ij} - M_W| < 10$ GeV on at least two pairs of jets (ij), as defined at the hadron level, the angular cuts of eq. (10) have also been implemented. The CM energy is $\sqrt{s} = 172$ GeV. Normalisation is to the total rates. Results are shown for the Durham algorithm, with $y_{\text{cut}} = 0.002$. Exactly four jets are required to be reconstructed. The bottom plot shows the ratio between the above two spectra.

interval	W^+W^- ME	QCD MEs	HERWIG	PYTHIA
χ_{BZ}				
$(75, 180)^\circ$	0.849	0.666	0.608	0.584
			0.596	0.574
$(100, 180)^\circ$	0.819	0.585	0.529	0.529
			0.492	0.495
$(125, 180)^\circ$	0.732	0.460	0.412	0.436
			0.361	0.388
Φ_{KSW}^*				
$(75, 180)^\circ$	0.896	0.748	0.708	0.718
			0.670	0.684
$(100, 180)^\circ$	0.827	0.641	0.601	0.614
			0.554	0.573
$(125, 180)^\circ$	0.666	0.485	0.446	0.468
			0.399	0.424
θ_{NR}^*				
$(0, 1)$	0.829	0.549	0.493	0.493
			0.476	0.471
$(0.25, 1)$	0.803	0.400	0.366	0.375
			0.355	0.359
$(0.5, 1)$	0.747	0.244	0.239	0.246
			0.238	0.242
θ_{34}				
$(-0.8, 0.8)$	0.785	0.635	0.565	0.529
			0.649	0.603
$(-0.6, 0.6)$	0.583	0.422	0.356	0.324
			0.442	0.400
$(-0.4, 0.4)$	0.384	0.266	0.219	0.199
			0.283	0.254
$e^+e^- \rightarrow 4 \text{ jets at LEP2}$				
$ M_{ij} - M_W < 10 \text{ GeV}$				

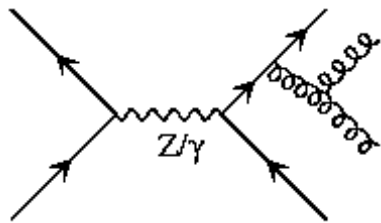
Tab. I



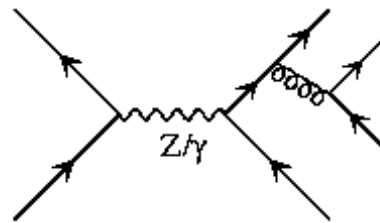
(a)



(b)



(c)



(d)

Fig. 1

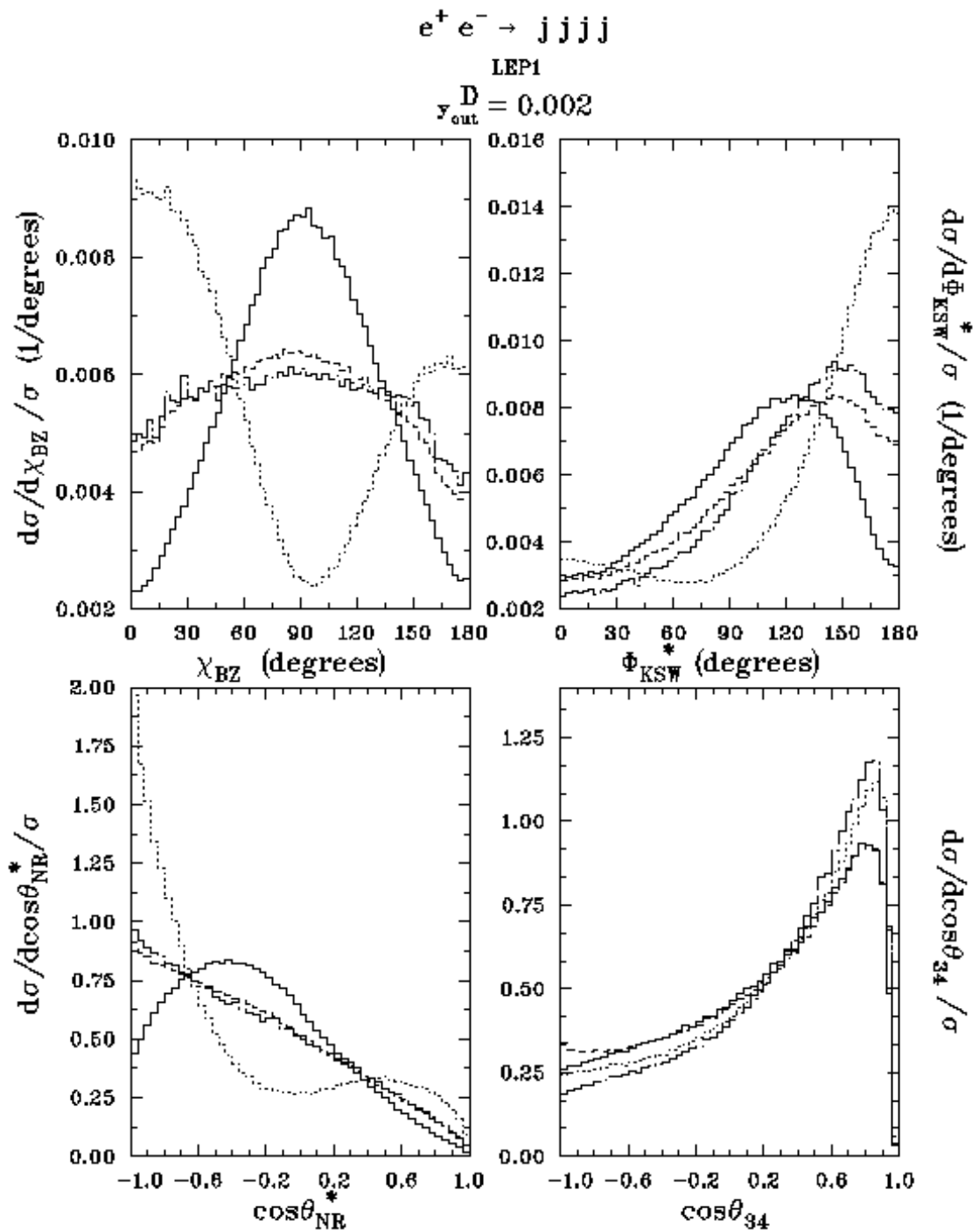


Fig. 2

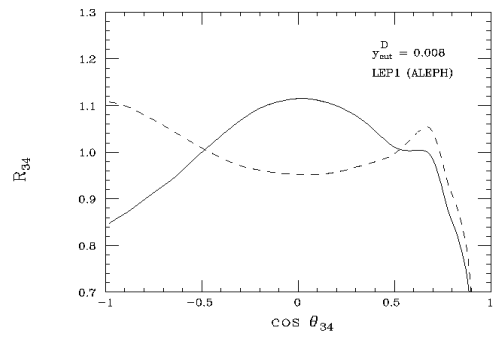
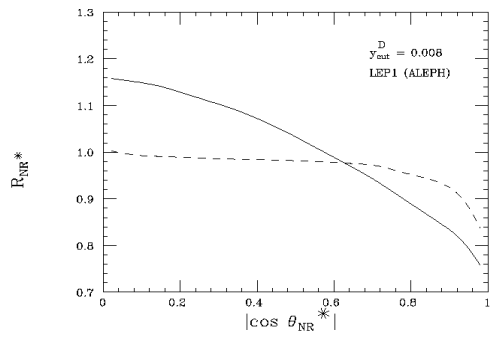
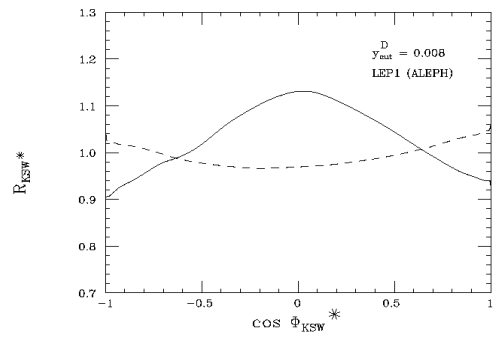
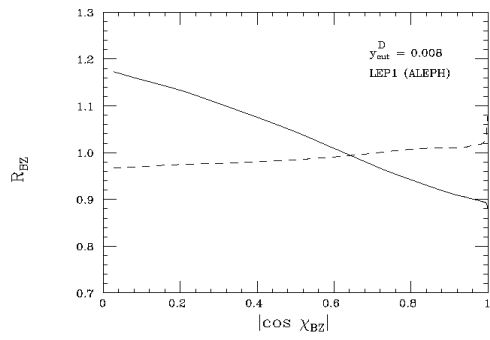


Fig. 3

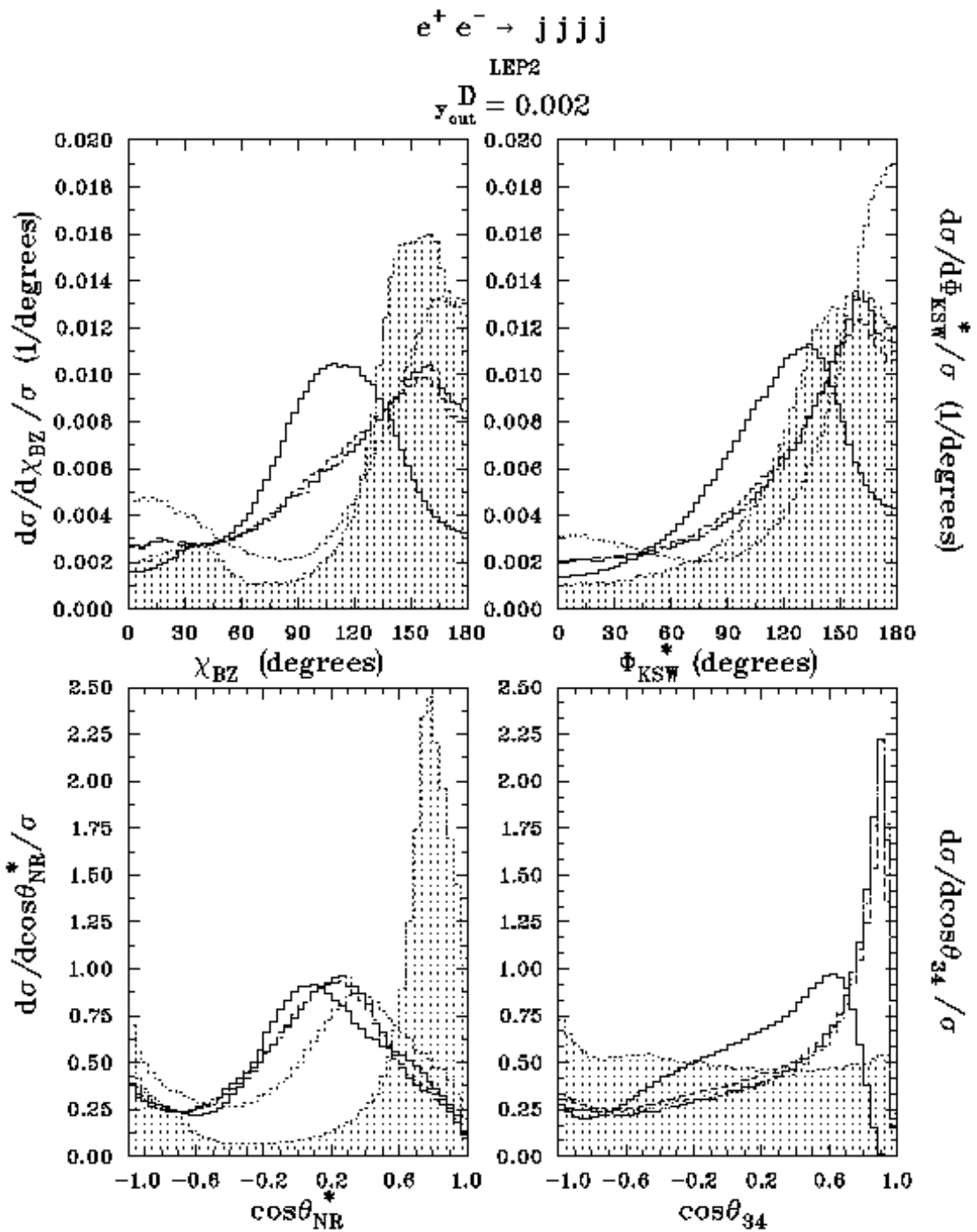


Fig. 4

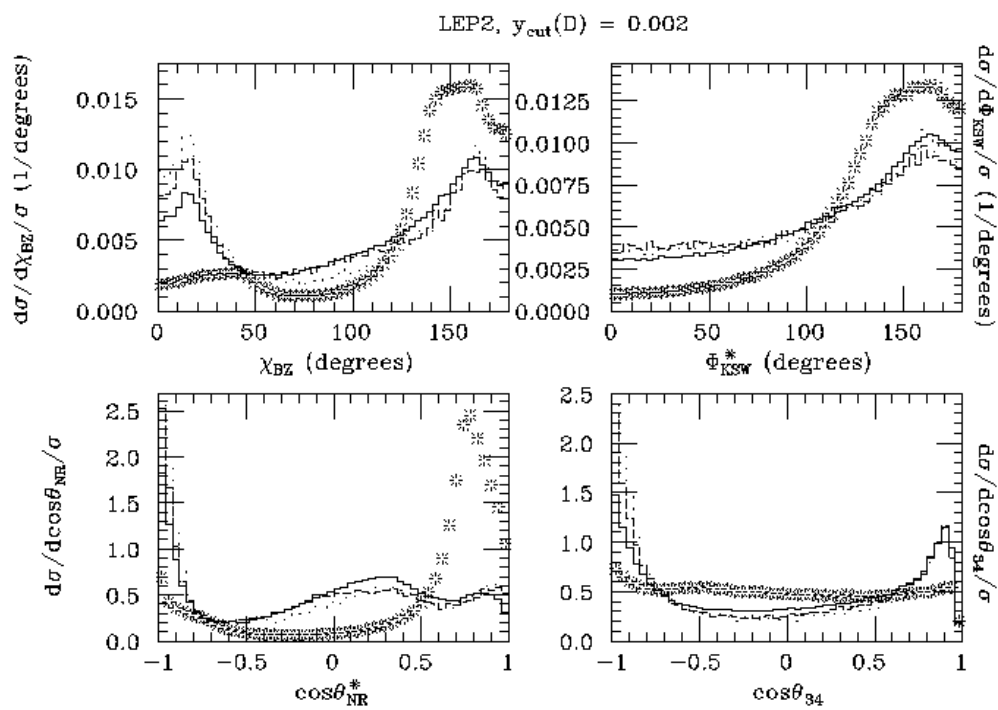


Fig. 5a

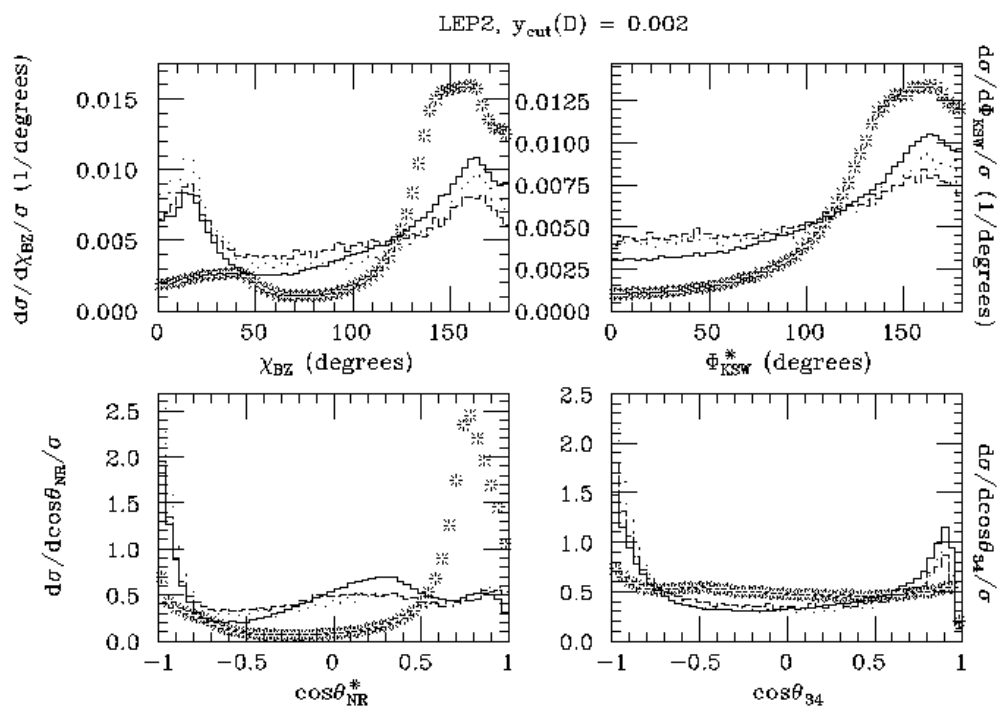


Fig. 5b

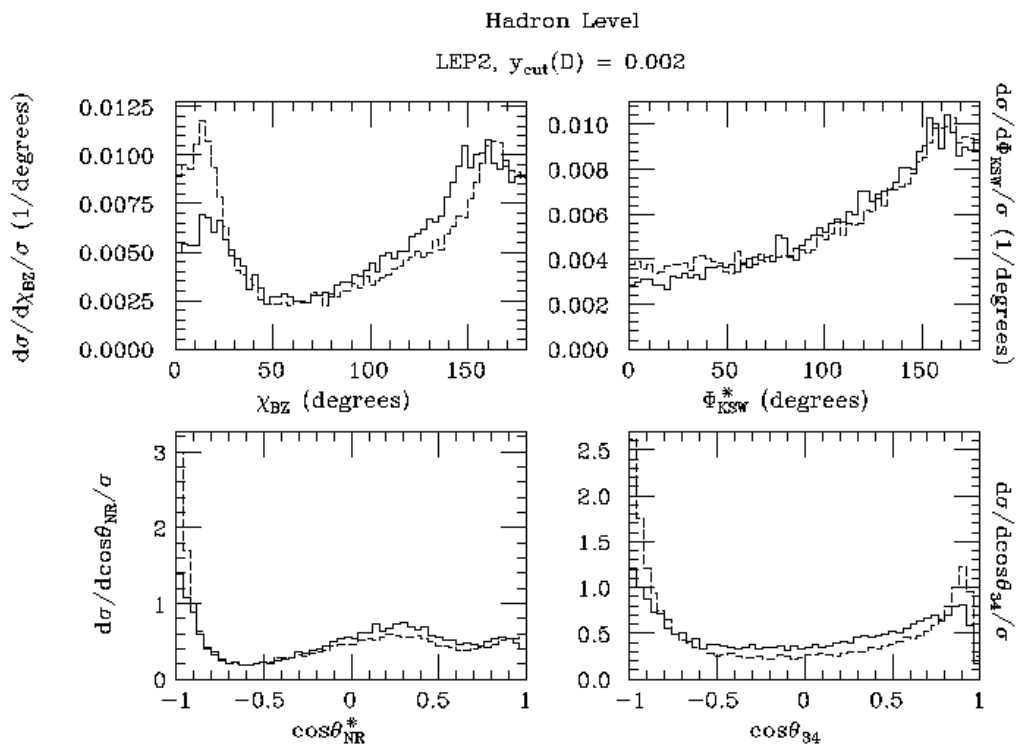


Fig. 6

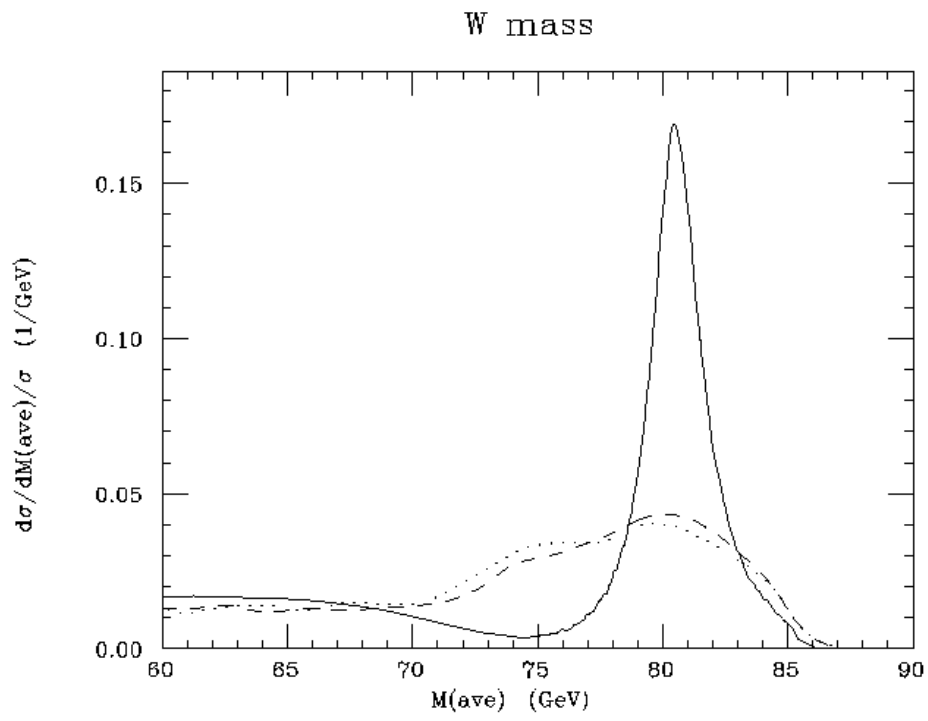


Fig. 7

W mass

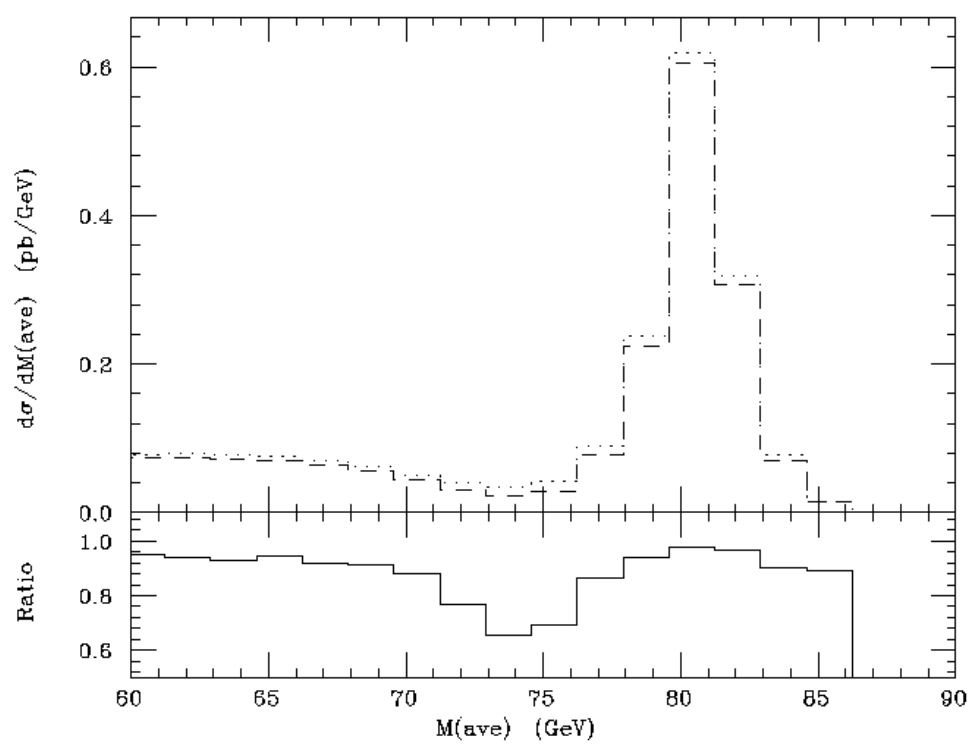


Fig. 8